

Structure and cooling of neutron stars: nuclear pairing and superfluid effects

F Isaule¹ and H F Arellano²

Departamento de Física-FCFM, Universidad de Chile, Avenida Blanco Encalada 2008, Santiago, Chile

E-mail: ¹fisaule@ing.uchile.cl, ²arellano@dfi.uchile.cl

Abstract. We investigate structure and cooling properties of neutron stars making use of microscopic descriptions of nuclear matter based on realistic nucleon-nucleon interactions. The equation of state is obtained from solutions of the Brueckner-Hartree-Fock equation for interacting nucleons at zero temperature. The structure aspects are described by the Tolman-Oppenheimer-Volkoff equation for hydrostatic equilibrium of non-rotating stars. Furthermore we have also solved Bardeen-Cooper-Schrieffer (BCS) pairing gap equations to identify superfluid states in neutronic matter. We obtain mass-radius behavior and cooling curves consistent with current understanding.

1. Introduction

Neutron stars are extremely dense and compact objects with mean mass density ranging between $2\rho_0$ and $3\rho_0$, where $\rho_0 = 2.8 \times 10^{14} \text{ g cm}^{-3}$ is the nuclear saturation density. Their masses are of the order of the solar mass while their radii are about 10 km. The inner layers of neutron star are governed by the equation of state (EoS) of dense matter, which is poorly known. For this reason neutron stars become a natural laboratory for nuclear physics. Observations of neutron star properties, like radius and surface temperature, provide valuable information to constrain the equation of state of nuclear matter [1].

New observations in the last few years have attracted much attention in the field. Observation of high-mass neutron stars may have ruled out soft equations of state for dense matter [2, 3]. Furthermore, the cooling of the neutron star in Cassiopeia A provides strong evidence for superfluidity in the star core [4], particularly in the $^3\text{PF}_2$ channel [5].

Here we report results for structure and cooling properties based on microscopic descriptions of nuclear matter. The equation of state of nuclear matter is based on solutions of the Brueckner-Hartree-Fock (BHF) equations for interacting nucleons in symmetric and neutronic matter at zero temperature [6], a reasonable starting point for ab-initio calculations. We use the Argonne v_{18} bare nucleon-nucleon (NN) interaction [7]. We calculate a equation of state for neutron star matter and obtain a mass-radius relation for non-rotating stars solving the Tolman-Oppenheimer-Volkoff (TOV) equations [8]. Furthermore, cooling curves for neutron stars using these results are calculated, including superfluid effects [9]. Pairing gaps in the 1S_0 and $^3\text{PF}_2$ channels are obtained solving the BCS gap equation [10].



2. Nuclear equation of state and neutron star structure

Infinite nuclear matter at zero temperature can be studied within the framework of the BHF approximation considering homogeneous matter in normal state. The effective interaction between pairs is described by the g matrix, which satisfies

$$g(\omega) = v + v \frac{Q}{\omega + i\eta - \hat{h}_1 - \hat{h}_2} g, \quad (1)$$

where v is the bare interaction between nucleons, \hat{h}_i the single-particle (sp) energy of nucleon i and Q the Pauli blocking operator. The solution of this equation allows the evaluation of the mass operator

$$M(k; E) = \sum_{|p| \leq k_f} \langle \frac{1}{2}(k-p) | g_K(E + e_p) | \frac{1}{2}(k-p) \rangle, \quad (2)$$

where $K = k + p$, is the total momentum, and

$$e_p = \frac{p^2}{2m} + U(p), \quad (3)$$

the sp energy. In the BHF approximation the sp potential is

$$U(k) = \text{Re} M(k; e_k). \quad (4)$$

Eqs. (1-4) are solved self-consistent following the *continuous choice* for $U(k)$ [11]. 1S_0 and 3SD_1 channels are treated following Ref. [12]. These considerations have led to coexisting solutions in symmetric matter which in this study appears to have negligible effects.

Self-consistent solutions for $U(k)$ at zero temperature were obtained using Argonne v_{18} potential. Solutions have been obtained for both symmetric and neutronic matter. In the case of symmetric nuclear matter (SMN) the Fermi momentum (k_F) ranges between 0.25 fm^{-1} and 2.2 fm^{-1} . In the case of pure neutronic matter (PNM) $k_f \leq 3 \text{ fm}^{-1}$. In Fig. 1 we show the binding energy per nucleon, B/A , as a function of density. It is observed the gas-like behavior of neutronic matter. In the case of SNM the saturation point occurs at $\rho = 0.25 \text{ fm}^{-3}$, with a binding energy per nucleon of -16.8 MeV.

2.1. Equation of state for beta-stable matter

The energy density for matter composed of interacting protons and neutrons, ultra-relativistic electrons and non-relativistic muons is given by [13]

$$\epsilon = \rho_p m_p c^2 + \rho_n m_n c^2 + B/A(\rho_p, \rho_n) \rho + \frac{(3\pi^2 \rho_e)^{5/3}}{5\pi^2} + \rho_\mu m_\mu c^2 + \frac{\hbar^2}{2m_\mu} \frac{(3\pi^2 \rho_\mu)^{5/3}}{5\pi^2}, \quad (5)$$

where $\rho = \rho_p + \rho_n$ is the nucleon density. In order to account for isospin asymmetry we introduce a parabolic approximation in terms of $\alpha = (\rho_n - \rho_p)/\rho$ [14]

$$B/A(\rho, \alpha) = (B/A)_{SNM}(\rho) + \alpha^2 [(B/A)_{PNM}(\rho) - (B/A)_{SNM}(\rho)]. \quad (6)$$

Here SNM and PNM refer to symmetric nuclear matter and pure neutron matter respectively. We use the B/A_{PNM} and B/A_{SNM} obtained from the self-consistent calculations we have performed. The pressure is given by

$$P = P_{\text{nucleons}} + P_{\text{leptons}}, \quad (7)$$

$$P_j = \rho_j^2 \frac{\partial}{\partial \rho_j} \left(\frac{\epsilon_j}{\rho_j} \right). \quad (8)$$

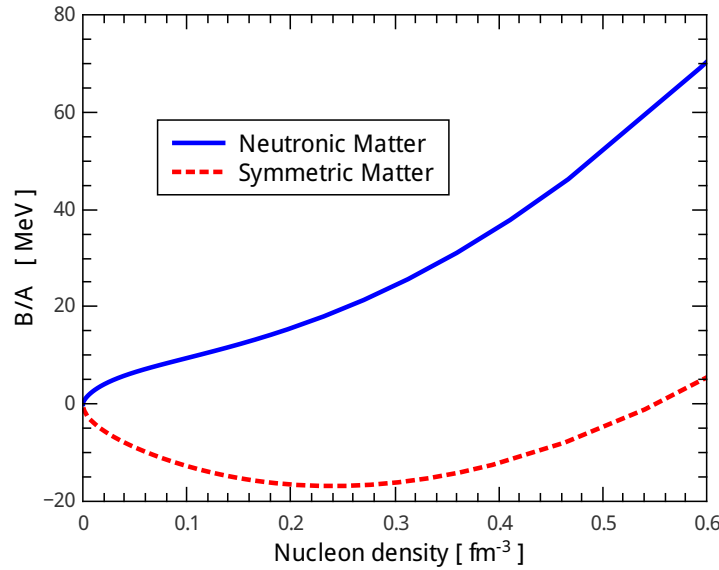


Figure 1. Energy per nucleon for symmetric (solid curve) and neutronic matter (dashed curve) based on the Argonne v_{18} potential.

Neutral beta-stable matter satisfies

$$\mu_n = \mu_p + \mu_e; \quad (9)$$

$$\rho_p = \rho_e + \rho_\mu; \quad (10)$$

$$\mu_e = \mu_\mu; \quad (11)$$

where $\mu_i = \partial \epsilon_i / \partial \rho_i$ represents the chemical potential of species i . Solving Eqs.(9)-(11) using Eq.(5) allows us to obtain the abundances of each specie ($\rho_i(\rho)$), hence the pressure as a function of the nucleon density $P(\rho)$ [15]. These considerations define the equation of state for beta-stable matter.

2.2. Neutron star structure

With a EoS for neutron star matter we are in condition to obtain the mass-radius behavior at equilibrium. To do so we solve the Tolman-Oppenheimer-Volkoff (TOV) equations for non-rotating stars,

$$\frac{dP(r)}{dr} = -\frac{Gm(r)\epsilon(r)}{r^2c^2} \left(1 + \frac{P(r)}{\epsilon(r)}\right) \left(1 + \frac{4\pi P(r)}{c^2m(r)}\right) \left(1 - \frac{2Gm(r)}{rc^2}\right)^{-1}, \quad (12)$$

$$\frac{dm(r)}{dr} = 4\pi r^2 \epsilon(r)/c^2, \quad (13)$$

where m is the enclosed mass up to a radius r and P is the local pressure. For the core of the star, where $\rho > \rho_0/5$, we have used the EoS for beta-stable matter obtained from the self-consistent calculations described above. For the crust and envelope we have used the EoS by Feynman-Metropolis-Teller [16], Haensel-Zdunik-Dobaczewski [17] and Negele-Vautherin [18]. We have solved these equations considering different central densities.

In Fig. 2 we show the behavior of the mass of a neutron star and its radius where equilibrium is imposed. As observed, we obtain a maximum mass of roughly $1.8 M_\odot$, not reaching the latest

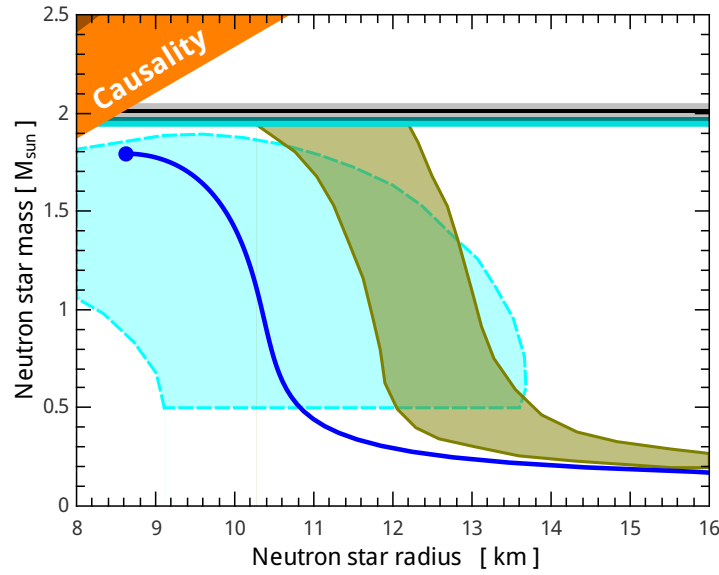


Figure 2. Neutron star mass expressed in solar mass units as a function of the star radius. The circle corresponds to the maximum mass reached within our approach. The brown region surrounded by solid lines is obtained from quiescent low-mass x-ray binary mass and radius observations [19]. The cyan region surrounded by dashed lines corresponds to the 90% confidence region for the mass-radius relation of NGC 6397 [20]. The two horizontal lines correspond to high mass neutron stars reported in Refs. [2, 3].

maximum masses observed of $2.1 M_{\odot}$ [2, 3]. However, this shortcoming is not unexpected considering the simplicity of the model, where three-body forces and sub-hadronic degrees of freedom in the inner core are not included.

3. Neutron star cooling

Recent developments in astronomical observations have allowed increasing precision in measurements of neutron stars properties. These observations provide important information regarding the cooling mechanisms, particularly about its superfluid and superconducting properties.

The cooling evolution of neutron stars can be obtained solving the general relativistic equations of thermal evolution [9, 21]

$$\frac{e^{-\lambda-2\Phi}}{4\pi^2} \frac{\partial}{\partial r} (e^{2\Phi} L_r) = -Q - \frac{c_T}{e^{\Phi}} \frac{\partial T}{\partial t} \quad (14)$$

$$\frac{L_r}{4\pi\kappa r^2} = e^{-\lambda-\Phi} \frac{\partial}{\partial r} (T e^{\Phi}), \quad (15)$$

where Q is the neutrino emissivity, κ is the thermal conductivity, L_r is the local luminosity and T is the temperature. The function Φ is related to the local pressure and energy density by

$$\frac{d\Phi}{dr} = -\frac{1}{\epsilon(r)} \frac{dP}{dr} \left[1 + \frac{P(r)}{\epsilon(r)} \right]^{-1}. \quad (16)$$

Additionally, $e^{-\lambda} = \sqrt{1 - 2Gm(r)/c^2 r}$.

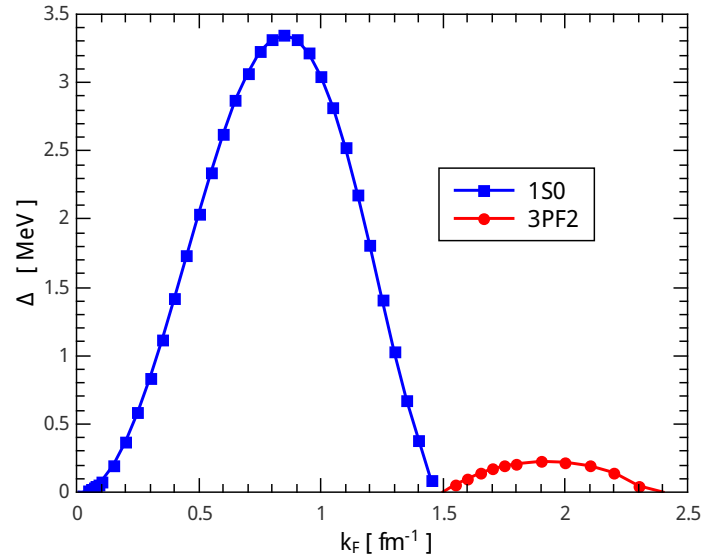


Figure 3. Energy gap as a function of the Fermi momentum in neutronic matter for channels 1S_0 and 3PF_2 .

We have solved Eqs. (14-15) using the code NSCool developed by D. Page [22]. Physical inputs such as neutrino emissivity, thermal conductivity and heat capacity are addressed in Refs. [21, 23]. We do not include internal heating, accretion, nor magnetic fields. The inputs are affected by superfluidity [24], a phenomenon which we are able to account for solving BCS gap equations in the 1S_0 and 3PF_2 channels in neutronic matter. To do so we have proceeded as in Ref. [12]. In this case the BCS gap equation for uncoupled channels is given by

$$\Delta(k) = - \sum_{k'} \langle k|U|k' \rangle \frac{\Delta(k')}{2E(k')}, \quad (17)$$

where $E(k)$ is the quasi-particle energy and

$$E(k) = \sqrt{\epsilon(k)^2 + |\Delta(k)|^2}; \quad \epsilon(k) = e(k) - \mu; \quad (18)$$

and $e(k)$ is the sp energy. Here μ represents the chemical potential. Analog equations are for NN coupled channels. In Fig. 3 we plot the pairing gap energies as a function of k_F for 1S_0 and 3PF_2 channels. It becomes evident that superfluidity in each channel occurs at non overlapping density domains. While 1S_0 superfluidity is restricted to $k_F \lesssim 1.5 \text{ fm}^{-1}$, superfluidity in the 3PF_2 channel occurs at k_F between 1.5 and 2.5 fm^{-1} , with a peak of 0.2 MeV at $k_F \sim 1.9 \text{ fm}^{-1}$ ($\rho \sim 1.6 \rho_0$).

We have studied the cooling evolution of a neutron star considering BHF solutions (accounting for dinucleons) and corresponding BCS gap solutions. In these calculations the critical temperature for superfluidity $T_c(k_F)$ is related to the gap energy at zero temperature by [25]

$$\frac{\Delta_{T=0}}{k_B T_c} \approx 1.764. \quad (19)$$

In Fig. 4 we plot the cooling curves for four neutron star masses. The rapid cooling of stars with $1.5 M_\odot$ and $1.6 M_\odot$ is triggered by the direct Urca process, which occurs only at high densities in the core of high-mass neutron stars. Our results suggest that the masses of the stars reported in Fig. 4 lie below $1.5 M_\odot$, a region governed by the modified Urca process.

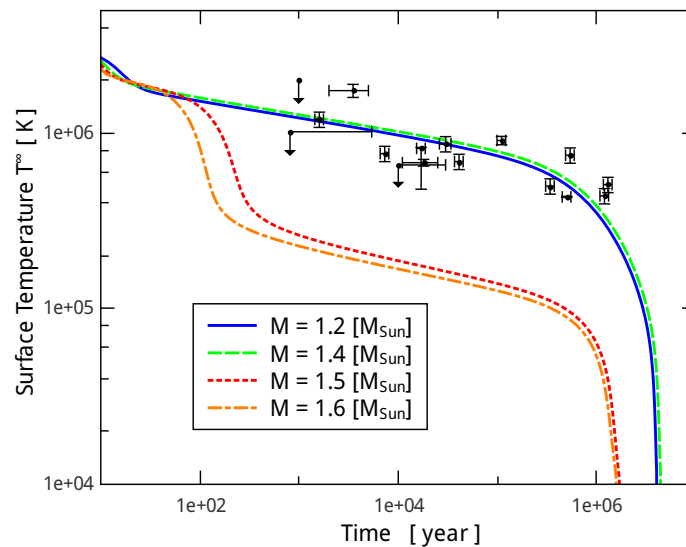


Figure 4. Surface temperature at infinity for three neutron star configurations with $^1\text{S}_0$ and $^3\text{P}_F$ superfluidity. The observations points are reported in Ref. [26].

4. Summary and conclusions

We have investigated static and cooling properties of neutron stars. Emphasis has been placed on a microscopic description of nuclear matter, including superfluid states. An EoS has been calculated using the Argonne AV18 bare NN interaction for both symmetric and pure neutron matter. BCS pairing gap based in the same bare interaction have been calculated and incorporated in the cooling codes. We reach a maximum mass for neutron stars around $1.8 M_{\odot}$. Cooling calculations show agreement between the observed temperature of neutron stars, as a function of time, if their masses lie below $1.5 M_{\odot}$. The inclusion of three-body forces are claimed to be important to account for the correct saturation density for symmetric nuclear matter and to reach higher masses for neutron stars. Current codes we have developed are being upgraded to include the chiral N3LO potential with N2LO three-body forces [27]. These developments shall allow us to investigate the implications of three-body forces on structure and cooling properties of neutron stars.

References

- [1] Haensel P, Potekhin A Y and Yakovlev D G 2007 *Neutron stars 1: Equation of state and structure* vol 326 (Springer Science & Business Media)
- [2] Antoniadis J *et al.* 2013 *Sci.* **340** 448, 1233232
- [3] Demorest P B, Pennucci T, Ransom S M, Roberts M S E and Hessels J W T 2010 *Nature* **467** 1081–1083
- [4] Page D, Prakash M, Lattimer J M and Steiner A W 2011 *Phys. Rev. Lett.* **106** 081101
- [5] Dong J M, Lombardo U and Zuo W 2013 *Phys. Rev. C* **87** 062801
- [6] Li Z H, Lombardo U, Schulze H J J, Zuo W, Chen L W and Ma H R 2006 *Phys. Rev. C* **74** 047304
- [7] Wiringa R B, Stoks V G J and Schiavilla R 1995 *Phys. Rev. C* **51** 38–51
- [8] Baldo M, Burgio G F and Bombaci I 1997 *Astron. Astrophys.* **328** 274–282
- [9] Page D, Geppert U and Weber F 2006 *Nucl. Phys. A* **777** 497–530
- [10] Dean D J and Hjorth-Jensen M 2003 *Rev. Mod. Phys.* **75** 607–656
- [11] Baldo M 1999 *Nuclear methods and the nuclear equation of state* vol 8 (World Scientific)
- [12] Arellano H and Delaroche J P 2015 *Eur. Phys. J. A* **51** 1–17
- [13] Blaschke D and Sedrakian D 2005 *Superdense QCD Matter and Compact Stars: Proceedings of the NATO Advanced Research Workshop on Superdense QCD Matter and Compact Stars* vol 197 (Springer Science & Business Media)

- [14] Vidaña I, Providência C, Polls A and Rios A 2009 *Phys. Rev. C* **80** 045806
- [15] Akmal A, Pandharipande V R and Ravenhall D G 1998 *Phys. Rev. C* **58** 1804–1828
- [16] Feynman R P, Metropolis N and Teller E 1949 *Phys. Rev.* **75** 1561–1573
- [17] Haensel P, Zdunik J L and Dobaczewski J 1989 *Astron. Astrophys.* **222** 353–357
- [18] Negele J W and Vautherin D 1973 *Nucl. Phys. A* **207** 298–320
- [19] Lattimer J M and Steiner A W 2014 *Astrophys. J.* **784** 123
- [20] Heinke C *et al.* 2014 *Mon. Not. R. Astron. Soc.* **444** 443–456
- [21] Gnedin O Y, Yakovlev D G and Potekhin A Y 2001 *Mon. Not. R. Astron. Soc.* **324** 725–734
- [22] Page D Nscool: A neutron star cooling code URL <http://www.astroscu.unam.mx/neutrones/NSCool/>
- [23] Yakovlev D G, Kaminker A D, Gnedin O Y and Haensel P 2001 *Phys. Rep.* **354** 1–155
- [24] Yakovlev D G, Kaminker A D and Levenfish K P 1999 *Astron. Astrophys.* **343** 650–660
- [25] Leggett A J 2006 *Quantum liquids: Bose condensation and Cooper pairing in condensed-matter systems* (Oxford University Press)
- [26] Yakovlev D G, Gnedin O Y, Kaminker A D and Potekhin A Y 2008 *AIP Conf. Proc.* **983** 379–387
- [27] Carbone A, Polls A and Rios A 2013 *Phys. Rev. C* **88** 044302

Acknowledgments

This work has been supported in part by FONDECYT under grant No 1120396. F. Isaule thanks CONICYT fellowship Beca Nacional, Contract No. 221320081.